

Polaron effect in GaAs-Ga_{1-x}Al_xAs quantum wells: A fractional-dimensional space approach

A. Matos-Abiague*

Max-Planck Institut für Mikrostrukturphysik, Weinberg 2, 06120 Halle, Germany

(Received 6 December 2001; published 5 April 2002)

The binding energy and the effective mass of a polaron confined in a GaAs-Ga_{1-x}Al_xAs quantum well are calculated within the framework of the fractional-dimensional space approach. In this scheme, the real confined “polaron plus quantum well” system is mapped onto an effective fractional-dimensional bulk in which the polaron behaves unconfined, and the fractional dimension is essentially related to the degree of confinement of the actual system. Analytical expressions allowing a very simple estimation of the corresponding polaron corrections are found. The fractional-dimensional theoretical results are shown to be in good agreement with previous more detailed calculations.

DOI: 10.1103/PhysRevB.65.165321

PACS number(s): 63.20.Kr, 71.38.-k

I. INTRODUCTION

With the progress in semiconductor growth techniques it has been possible to produce a variety of low-dimensional systems such as quantum wells (QW's), superlattices, quantum wires, and quantum dots. These systems exhibit a set of interesting physical properties that have found applications in a wide range of electronic and optoelectronic devices. Consequently, in the last decades a great deal of research effort has been devoted to the study of the physical effects occurring in such low-dimensional systems. One of the effects that has attracted the attention of a considerable amount of researchers is the polaron effect.

In particular, some commonly used QW's, such as GaAs-Ga_{1-x}Al_xAs, are constituted by weak polar semiconductors in which the polaron effects can strongly influence the optical and transport properties of the heterostructure. Indeed, the electron-LO-phonon interaction leading to the polaron effect modifies the properties of the electron confined in the QW.

At earlier stages, polarons in bulk material were investigated and a wide variety of mathematical techniques were applied to the study of the polaron problem (see, for instance, Refs. 1 and 2). The polaron confined to an infinite thin two-dimensional (2D) layer was firstly studied by Das Sarma and Mason.³ Polaron corrections in an infinitely deep QW of a finite length were calculated in Refs. 4–6. In these papers only the interaction with the bulk LO-phonon modes was considered. The polaron effect in heterostructures of finite size is, however, quite different from that in bulk materials. In the former case a variety of phonon modes (e.g., bulklike phonon modes,⁷ slab modes,^{8–10} interface modes,^{7–9,11–13} half-space modes^{11–13}) arises as a consequence of the presence of the heterointerfaces. Consequently, a rigorous treatment of the electron-phonon interaction in semiconductor heterostructures requires the consideration of all these modes. The polaron problem in QW's becomes then too complicated and even the simplest models cannot be resolved analytically. For the influence of the different phonon modes on polarons in different layered heterostructures see, for instance, Refs. 14–20.

In order to simplify the polaron problem in multilayered heterostructures, Smondyrev, Gerlach, and Dzero²¹ have recently proposed a simplified polaron model that takes into

account the finite size of the QW and the finite height of the confinement potential and deals with only one bulk phonon mode. The purpose of the present paper is to go one step forward and to formulate a more simplified model to calculate, in a purely analytical way, the polaron corrections in GaAs-Ga_{1-x}Al_xAs quantum wells, within a good accuracy.

Of particular interest to the present work is the original approach proposed by He.^{22,23} In this approach the anisotropic (or confined) interactions in real 3D space are treated as isotropic (or unconfined) ones in an effective fractional-dimensional environment the dimension of which constitutes a measure of the degree of anisotropy (or confinement) of the actual physical system. The main advantage of this approach lies in the fact that all information about a perturbation (confinement or anisotropy) can be introduced in a single value—the dimensionality. Thus, given this simple value, the real system can be modeled in a simple analytical way. In the last years, the fractional-dimensional space approach has been successfully used in modeling exciton,^{24–28} magnetoexciton,^{29,30} biexciton,^{31,32} and impurity states^{27,33,34} in semiconductor heterostructures. The Stark shift of excitonic complexes³⁵ and the refractive index³⁶ in quantum well structures have also been studied within the fractional-dimensional space approach.

In the present paper we extend the fractional-dimensional space formalism to the case of a polaron confined to a rectangular quantum well. Thus, the real confined “polaron + quantum well” system is mapped onto an effective fractional-dimensional bulk in which the polaron behaves unconfined, and the fractional dimension is essentially related to the degree of confinement of the actual system. The paper is organized as follows. For completeness of argument we briefly comment on some results of a previous work³⁷ in Sec. II, where the Fröhlich-like Hamiltonian describing the electron-LO-phonon interaction in a fractional-dimensional space is presented. The corresponding fractional-dimensional polaronic corrections in the weak-coupling limit are obtained in Sec. III, within second-order perturbation theory. In Sec. IV the polaron binding energy and effective mass in an infinitely deep rectangular quantum well are obtained for varying well width. The results are compared with the calculations reported in Ref. 16. In Sec. V the polaron problem in GaAs-Ga_{1-x}Al_xAs quantum wells is considered and a com-

parison of our results with calculations by other authors is shown. Finally, conclusions are summarized in Sec. VI.

II. THE FRACTIONAL-DIMENSIONAL ELECTRON-PHONON HAMILTONIAN

The first difficulty arising in dealing with the fractional-dimensional formalism is that the fractional-dimensional space is not, in general, a vector space.³⁸ However, one can trace a certain number of mutually perpendicular lines. A remarkable fact is that, for noninteger values of the dimension D of the space, the largest number s of mutually perpendicular lines can even be greater than D (see Ref. 38). Of course, when D is an integer we have $D=s$. The set of s mutually perpendicular lines can then be regarded as a set of orthogonal axes along which we can define certain *pseudocoordinates*. Thus, it is possible to describe the position of the electron by introducing an s -component *pseudovector* \mathbf{r} . In the same way we can define the wave *pseudovectors* \mathbf{q} and \mathbf{k} corresponding to the phonons and the electron, respectively. The Fröhlich-like Hamiltonian that describes the electron-phonon interaction in a fractional-dimensional space can then be written as

$$\hat{H}_{e-ph} = \sum_{\mathbf{q}} [C_{\mathbf{q}}(D)\hat{b}_{\mathbf{q}}\exp(i\mathbf{q}\cdot\mathbf{r}) + C_{\mathbf{q}}^*(D)\hat{b}_{\mathbf{q}}^\dagger\exp(-i\mathbf{q}\cdot\mathbf{r})], \quad (1)$$

where $b_{\mathbf{q}}^\dagger$ ($b_{\mathbf{q}}$) is the creation (annihilation) operator for a phonon with wave *pseudovector* \mathbf{q} , and $C_{\mathbf{q}}(D)$ is the fractional-dimensional coupling coefficient of the electron-phonon interaction.

By considering that the basic interaction characterizing the electron motion in N dimensions (N being an integer number) remains Coulomb-like ($\sim 1/r$), Peeters, Xiaoguang, and Devreese³⁷ obtained an expression for the N -dimensional coupling coefficient of the electron-phonon interaction. Although the procedure used by these authors is valid only for integer values of the dimension,³⁹ one can try a straightforward generalization of the results in Ref. 37 by extending N to noninteger values. At first sight, this prolongation of N to noninteger values in order to obtain the corresponding fractional-dimensional coupling coefficient may seem not quite convincing. Nevertheless, it gives the appropriate fractional-dimensional coupling coefficient as will be shown. Actually, the axiomatic nature of the fractional-dimensional spaces is different from that of integer-dimensional ones and we cannot expect that this simple procedure will conduce always to the correct fractional-dimensional values (a brief comment about this situation can be found also in Ref. 40). In this sense, the dependence of the fractional-dimensional quantities on the dimension of the space is not a trivial dependence; i.e., although the fractional-dimensional expressions recover the corresponding integer-dimensional ones when the dimension becomes an integer number, the opposite is not true in general. In the present problem, however, the simple extension of N in the coupling coefficient obtained in Ref. 37 to noninteger values gives the appropriate expression corresponding to the fractional-dimensional case.

In fact, following the same physical considerations as in Ref. 37, but now assuming a fractional dimension (and this implies to renounce the use of any vector property), one can obtain

$$C_{\mathbf{q}}(D) = -i\hbar\omega_{LO} \left(\frac{F_D(q)\alpha}{V_D} \right)^{1/2} \left(\frac{\hbar}{2m\omega_{LO}} \right)^{1/4}, \quad (2)$$

where

$$F_D(q) = (2\pi)^{D/2} \int_0^\infty dr r^{D-1} (qr)^{1-D/2} J_{D/2-1}(qr) \frac{1}{r} \quad (3)$$

is the fractional-dimensional Fourier transform³⁸ of the Coulomb-like potential. In the equations above and in what follows m , α , and ω_{LO} represent the electron effective mass, the Fröhlich constant, and the bulk LO-phonon limiting frequency, respectively, V_D is the fractional-dimensional volume of the crystal to which Born-Von Karman periodicity conditions are applied, and $J_\nu(x)$ represent the Bessel functions. Notice that introducing the fractional-dimensional Fourier transform we avoid the use of any property concerning vector spaces.

After the corresponding integration in Eq. (3) we obtain from Eq. (2) the coupling coefficient

$$C_{\mathbf{q}}(D) = -i\hbar\omega_{LO} \left[\frac{(4\pi)^{(D-1)/2} \Gamma[(D-1)/2] \alpha}{q^{D-1} V_D} \right]^{1/2} \times \left(\frac{\hbar}{2m\omega_{LO}} \right)^{1/4}, \quad (4)$$

characterizing the electron-phonon interaction in the fractional-dimensional bulk. We remark that if we extend the values of the dimensional parameter to noninteger values in the results of Ref. 37, we obtain an expression for the coupling coefficient that coincides precisely with Eq. (4).

III. FRACTIONAL-DIMENSIONAL POLARONIC CORRECTIONS

Taking into account that in GaAs-Ga_{1-x}Al_xAs quantum wells the electron-phonon coupling constant $\alpha \ll 1$ we can restrict our study to the weak-coupling case.

The electron self-energy due to the electron-LO-phonon interaction in the weak-coupling approximation can be calculated within second-order perturbation theory. The energy of a fractional-dimensional polaron in the ground state is given by

$$E = E_{\mathbf{k}}^{(0)} + \sum_{\mathbf{k}'} \frac{|\langle 1_{\mathbf{k}'}, 0_{\mathbf{k}}, 1_{\mathbf{q}} | \hat{H}_{e-ph} | 0_{\mathbf{k}'}, 1_{\mathbf{k}}, 0_{\mathbf{q}} \rangle|^2}{\bar{E}_{\mathbf{k}} - \bar{E}_{\mathbf{k}'}} \quad (5)$$

where

$$\bar{E}_{\mathbf{k}} = \langle 0_{\mathbf{q}}, 1_{\mathbf{k}}, 0_{\mathbf{k}'} | \hat{H}^{(0)} | 0_{\mathbf{k}'}, 1_{\mathbf{k}}, 0_{\mathbf{q}} \rangle = E_{\mathbf{k}}^{(0)} \quad (6)$$

and

$$\bar{E}_{\mathbf{k}'} = \langle 1_{\mathbf{k}'}, 0_{\mathbf{k}}, 1_{\mathbf{q}} | \hat{H}^{(0)} | 1_{\mathbf{q}}, 0_{\mathbf{k}}, 1_{\mathbf{k}'} \rangle = E_{\mathbf{k}'}^{(0)} + \hbar\omega_{LO} \quad (7)$$

are the unperturbed electron energies corresponding to the initial and intermediate states, respectively.

In the equations above $|0_{\mathbf{k}',1_{\mathbf{k}},0_{\mathbf{q}}}\rangle$ denotes the initial state with one electron in the state \mathbf{k} , zero electrons in the \mathbf{k}' , and zero phonons. The assumption of absence of phonons in the initial state is usually fulfilled for low temperatures. The interpretation of the intermediate states $|1_{\mathbf{q}},0_{\mathbf{k}},1_{\mathbf{k}'}\rangle$ is analogous to that of the initial states.

Taking into account that the free electron motion in a fractional-dimensional space can be described by a plane wave³⁸ and after the corresponding integration over the volume V_D in the matrix elements present in Eq. (5) we get

$$E - E_{\mathbf{k}}^{(0)} = \frac{2m}{\hbar^2} \sum_{\mathbf{k}',\mathbf{q}} \frac{|C_{\mathbf{q}}(D)|^2 |\Delta[\mathbf{k}' - \mathbf{k} + \mathbf{q}]|^2}{k^2 - k'^2 - R_p^{-2}}, \quad (8)$$

where $R_p = \sqrt{2m\omega_{LO}/\hbar}$ is the polaron radius and $\Delta(x)$ represents the Kronecker delta function [$\Delta(x) = 1$ if $x = 0$, and $\Delta(x) = 0$ if $x \neq 0$]. This function, as in the integer-dimensional bulk case, is an expression of the momentum conservation law.

By now approximating the summation over \mathbf{q} in Eq. (8) by an integral

$$\begin{aligned} \sum_{\mathbf{q}} \dots &\approx \frac{V_D}{(2\pi)^D} \frac{2\pi^{(D-1)/2}}{\Gamma[(D-1)/2]} \\ &\times \int_0^\infty \int_0^\pi \dots q^{D-1} (\sin \theta)^{D-2} dq d\theta, \end{aligned} \quad (9)$$

and after the standard procedures, we obtain from Eq. (8) the following expression for the polaron energy:

$$E = -\alpha \hbar \omega_{LO} G_\alpha(D) + \frac{\hbar^2 k^2}{2m^*}, \quad (10)$$

where

$$m^* = \frac{m}{1 - \alpha G_\beta(D)} \quad (11)$$

is the polaron effective mass.

In Eqs. (10) and (11) the D -dependent functions $G_\alpha(D)$ and $G_\beta(D)$ are given by

$$G_\alpha(D) = \frac{\sqrt{\pi}}{2} \frac{\Gamma[(D-1)/2]}{\Gamma[D/2]} \quad (12)$$

and

$$G_\beta(D) = \frac{\sqrt{\pi}}{4} \frac{\Gamma[(D-1)/2]}{D\Gamma[D/2]}, \quad (13)$$

respectively. In Eqs. (9), (12), and (13), $\Gamma(x)$ represents the gamma function.

The set of equations (10)–(13) determines the polaronic corrections in a fractional-dimensional bulk. It is straightforward to check that these equations recover the well-known forms in both the exact 2D and 3D limits.

IV. POLARON IN AN INFINITE-BARRIER QUANTUM WELL

In the present section we will study the behavior of the polaron confined in an infinitely deep quantum well, within the framework of the fractional-dimensional space approach. In this approach the real three-dimensional ‘‘polaron + QW’’ system will be treated as a polaron in an effective fractional-dimensional bulk, which dimension constitutes a measure of the degree of confinement of the real system. Thus, given the value of the dimensionality of the effective bulklike environment, the corresponding polaron corrections can be easily obtained from Eqs. (10) and (11). The question that arises is then how to calculate the appropriate value of the dimensional parameter. At earlier stages, Mathieu and co-workers introduced a heuristic model for calculating the appropriate dimensionality in the case of confined excitons. Their method provide a surprisingly accurate parametrization of the exciton binding energy in rectangular quantum wells,²⁴ quantum well wires,²⁵ and superlattices.²⁶ More recently de Dios-Leyva and co-workers²⁷ have developed a systematic procedure for determining the dimensionality of the effective medium in modeling exciton and impurity states in quantum wells,^{27,28} multiple quantum wells,³³ and superlattices.³⁴ For the sake of simplicity we will consider in the present paper a procedure analogue to that in Refs. 24–26.

Following Christol *et al.*,²⁵ since the dimensional parameter is a measure of the degree of confinement of the real system embedded in a three-dimensional Euclidean space, it can be determined by

$$D = \beta_x + \beta_y + \beta_z, \quad (14)$$

where β_x , β_y , and β_z represent the ratios of the homothetic reduction of the unit length for the directions x , y , and z , respectively.

In the case of a rectangular quantum well grown along the z direction, the motion in the (x,y) plane is free and we get $\beta_x = \beta_y = 1$. The ratio of the homothetic reduction of the unit length in the z direction produced by the confinement effects can be calculated through the relation

$$\beta_z = 1 - \exp[-\xi], \quad (15)$$

where

$$\xi = \frac{\text{length of confinement}}{\text{effective characteristic length of interaction}}. \quad (16)$$

Equations (14)–(16) have been successfully used in modeling exciton states in semiconductor quantum wells.^{24,25} In the case of an exciton confined in an infinitely deep quantum well we have, for instance, $\xi = L_w/(2a_0)$ (see Ref. 24), where L_w represents the well width and a_0 is the effective Bohr radius of the three-dimensional exciton. The dimensionality is then given by $D = 3 - \exp[-\xi]$.

Let us consider now a polaron confined in an infinitely deep rectangular quantum well. In this case, the electron is restricted to move only inside the well; consequently, the length of confinement is equal to the well width. On the

other hand, the effective characteristic length of the electron-phonon interaction is equal to the polaron diameter

$$d = 2R_p = 2 \sqrt{\frac{\hbar}{2m\omega_{LO}}}. \quad (17)$$

Therefore, the dimensional parameter can be calculated through the simple relation

$$D = 3 - \exp\left[-\frac{L_w}{2R_p}\right], \quad (18)$$

where R_p is the polaron radius.

By now substituting the equation above in Eqs. (10)–(13) we can estimate in a very simple way the energy and the effective mass of the confined polaron. We use in our calculations the same material parameters as in Ref. 16. The numerical results are shown in Fig. 1.

The well width dependence of the fractional-dimensional polaron binding energy compared with the corresponding calculations by Hai, Peeters, and Devreese¹⁶ is displayed in Fig. 1(a). An excellent agreement between our results and those reported in Ref. 16 for 3D bulk LO-phonon modes can be clearly appreciated. Notice that in Fig. 1(a) the polaron binding energy is given in units of the 2D polaron binding energy limit, i.e., $\Delta E_r = \Delta E / \Delta E_{2D}$. An overall agreement between our results and those reported in Ref. 16 can be appreciated in Fig. 1(b) for the well width dependence of the polaron effective mass. Here the polaron effective mass has also been referred to its 2D value, i.e., $\Delta m_r = \Delta m / \Delta m_{2D}$.

The fractional-dimensional parameter corresponding to the results shown in Figs. 1(a) and 1(b) is displayed in Fig. 1(c) as a function of the well width. A transition from the 2D limit to the 3D limit when the well width increases is quite apparent. In fact, for $L_w \geq 300$ Å the effective system becomes practically three dimensional.

It is worth remarking that in Figs. 1(a) and 1(b) we compare our results with those results reported in Ref. 16 that correspond only to the bulklike phonon case. One cannot expect that in the region of narrow wells the approach proposed in the present section will give correct values for the polaronic corrections corresponding to the interface and slab phonon modes. We have assigned to the effective fractional-dimensional bulk a fix set of material parameters equal to that of GaAs layer. Thus, for wide quantum wells the model presented in this section gives the correct limit values of the polaronic corrections (i.e., those corresponding to a GaAs bulk). However, for narrow quantum wells the correct limit corresponding to a GaAs-Ga_{1-x}Al_xAs bulk cannot be recovered. In order to take account of these effects the fractional-dimensional model is generalized to the case of a finite-barrier quantum well in the next section.

V. POLARON IN A FINITE-BARRIER QUANTUM WELL

We consider now the problem of a polaron confined in a semiconductor GaAs-Ga_{1-x}Al_xAs QW grown along the z direction. Within the effective mass and parabolic band approximations the electronic part of the Hamiltonian may be a given, in the growth direction, by

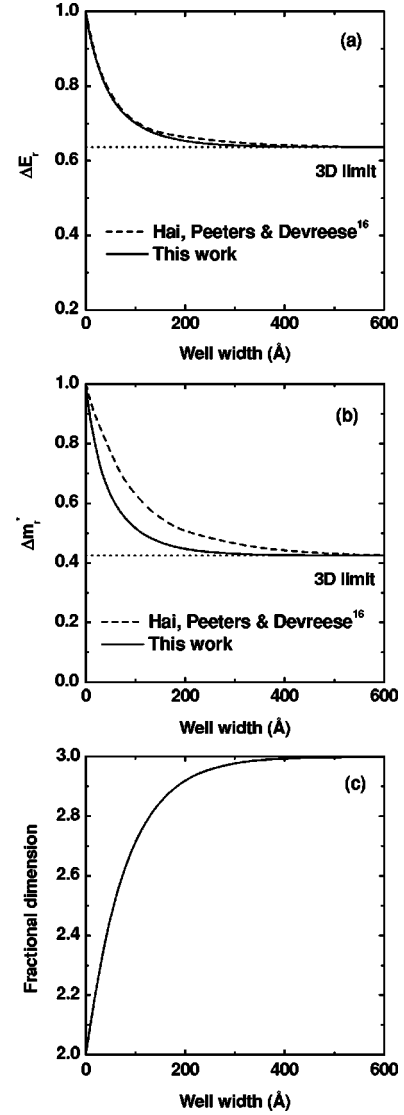


FIG. 1. Well width dependence of the polaron binding energy (a), the polaron effective mass (b), and the corresponding fractional dimension (c), for a polaron confined in an infinite rectangular quantum well. Both the polaron binding energy and the effective mass are referred to their corresponding 2D values. Solid curves correspond to the present fractional-dimensional results and the dashed lines to calculations by Hai, Peeters, and Devreese (Ref. 16).

$$\hat{H}_e = -\frac{\hbar^2}{2} \frac{d}{dz} \left(\frac{1}{m(z)} \frac{d}{dz} \right) + V(z), \quad (19)$$

where

$$V(z) = \begin{cases} 0 & \text{if } |z| \leq L_w/2, \\ V_0 & \text{otherwise.} \end{cases} \quad (20)$$

In the equations above and in what follows $m(z)$ represents the z -dependent effective mass of the electron, L_w is the well width, and V_0 is the height of the potential barrier (notice that the value of V_0 depends on the Al concentration in the barrier).

While in the infinitely deep QW the length of confinement l can be taken equal to the well width (see the previous section), in the present problem the motion of the electron is no longer restricted to the region inside the well only. Therefore, the spreading of the electron wave function into the barriers on both sides of the well has to be considered in defining the corresponding length of confinement. Taking into account that the spatial extension of the electron motion in the barrier region is mainly characterized by $(k_{out}^{-1} + k_{out}^{-1})$, we can define the length of confinement as follows:

$$l = L_w + \frac{2}{k_{out}}, \quad (21)$$

where

$$k_{out} = \sqrt{\frac{m_{out}}{m_{in}} \left(\frac{2m_{in}\hbar V_0}{L_w} - E_1 \right)} \quad (22)$$

represents the electron wave vector in the barrier region, E_1 being the electron eigenenergy determined by \hat{H}_e [see Eq. (19)] and corresponding to the first subband (notice that we are interested in the polaron ground state only). In Eq. (22) and in what follows, the subindexes *in* and *out* are labels for the well and barrier regions, respectively.

In a GaAs-Ga_{1-x}Al_xAs QW the material parameters that characterize the polaron properties differ when passing from the well to the barrier region. In order to take account of this fact, we may assign to the effective fractional-dimensional bulk an average of the material parameters over the polaron positions. If we consider the polaron as a phonon cloud around the electron, the polaron position will be determined, essentially, by the electron position. The mean values of the material parameters can therefore be calculated in the same manner as in Ref. 21, i.e., according to the way they enter in the Hamiltonian of the system and weighting the spatial integration with the square module of the electron ground-state wave function $\Psi(z)$ determined by \hat{H}_e [Eq. (19)]. Our effective fractional-dimensional bulk is then characterized by the following set of mean parameters:

$$m^{-1} = \int_{-\infty}^{\infty} \frac{1}{m(z)} |\Psi(z)|^2 dz, \quad (23)$$

$$\omega_{LO} = \int_{-\infty}^{\infty} \omega_{LO}(z) |\Psi(z)|^2 dz, \quad (24)$$

and

$$\sqrt{\alpha} = \int_{-\infty}^{\infty} \frac{\omega_{LO}(z)}{\omega_{LO}} \left(\alpha(z) \sqrt{\frac{m\omega_{LO}}{m(z)\omega_{LO}(z)}} \right)^{1/2} |\Psi(z)|^2 dz. \quad (25)$$

In the same way, the mean polaron radius that determines the effective characteristic length of the electron-phonon interaction can be written as

$$\sqrt{R_p} = \int_{-\infty}^{\infty} \frac{\omega_{LO}(z)}{\omega_{LO}} \sqrt{\frac{\alpha(z)R_p(z)}{\alpha}} |\Psi(z)|^2 dz. \quad (26)$$

Notice that in our model the electron effective mismatch is included in the electron wave function $\Psi(z)$. That is, in our model the function $\Psi(z)$ does not depend on the mean value of the electron effective mass but on m_{in} and m_{out} . Therefore, the mean value m can be determined directly from Eq. (23), avoiding the self-consistent procedure required in Ref. 21.

Finally, after considering Eqs. (14)–(16) and (21), the dimension corresponding to the effective bulklike environment can be calculated as

$$D = 3 - \exp\left[-\frac{(2+k_{out}L_w)}{2k_{out}R_p} \right], \quad (27)$$

and the polaronic corrections can be obtained in a very simple analytical way from Eqs. (10)–(13).

The fractional-dimensional polaron binding energy (solid line) as a function of the well width for a GaAs-Ga_{0.7}Al_{0.3}As rectangular quantum well is displayed in Fig. 2(a). For very narrow quantum wells the polaron binding energy has the value corresponding to the 3D limit of a GaAs-Ga_{0.7}Al_{0.3}As bulk. The polaron energy shift then decreases as the well width increases and reaches a minimum at $L_w \sim 2$ Å [see the inset in Fig. 2(a)]. By continuing to increase the well width, the energy shift increases and reaches a maximum at $L_w \sim 10$ Å. For wider quantum wells the energy shift again decreases as L_w increases and recovers the appropriate 3D limit value corresponding to a GaAs bulk for very large well widths ($L_w > 300$ Å). A similar behavior for the fractional-dimensional polaron effective mass can be appreciated in Fig. 2(b), where the well width dependence of the mass shift $\delta m = \Delta m / \Delta m_{in}$ is displayed. Notice that, actually, δm represents the ratio of the mass shift (Δm) to that in the well material (Δm_{in}). Comparing our results (solid line) with those reported by Smodyrev, Gerlach, and Dzero²¹ (dashed line) good agreement is found. The maximal discrepancy between both calculations is about 3.5% (0.15 meV) for the energy shift and about 12% for the mass shift. For Fig. 2 we have used the same set of material parameters as defined by Smodyrev, Gerlach, and Dzero in Ref. 21.

In Fig. 2(c) we show the well width dependence of the dimensional parameter corresponding to the fractional-dimensional results in Figs. 2(a) and 2(b). For large well widths the system behaves as a GaAs bulk and consequently the dimensional parameter has the limit value $D = 3$. When the well width decreases, the system becomes more and more confined, the polaron turns more *compressed*, and the effective dimension decreases, reaching a minimum for $L_w \approx 25$ Å. If we continue decreasing the well width, the tunneling through the well barriers becomes significant and the degree of confinement of the system decreases. Consequently, the corresponding fractional dimension increases and recovers a value of 3 for very narrow quantum wells.

Although Fig. 2 shows an overall quantitative agreement between our results and the calculations by Smodyrev, Gerlach, and Dzero,²¹ there is, however, a significant qualitative difference. While in Ref. 21 these authors obtained only a peak in the well width dependence of both the energy and the mass shifts [notice that in Fig. 2(a) the peak in the

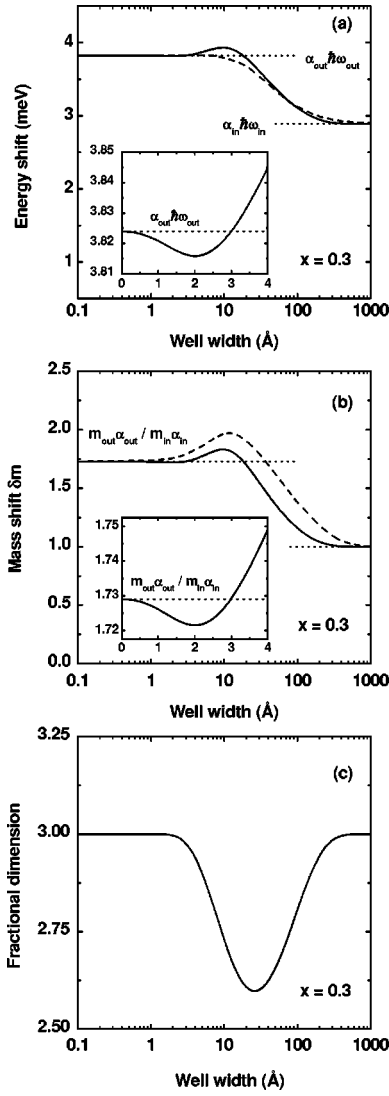


FIG. 2. Well width dependence of the polaron energy shift (a), the polaron mass shift (b), and the corresponding fractional dimension (c) for a polaron confined in a GaAs-Ga_{0.7}Al_{0.3}As rectangular quantum well. Solid curves correspond to the present fractional-dimensional results and the dashed lines to calculations by Smondyrev, Gerlach, and Dzero (Ref. 21). The insets show a zoom-in of the corresponding fractional-dimensional polaronic corrections. The material parameters have been assumed as defined by Smondyrev, Gerlach, and Dzero in Ref. 21.

energy shift reported in Ref. 21 is very small and almost invisible], a structure with a peak and a dip [see Figs. 2(a) and 2(b), and the corresponding insets] is obtained within the present fractional-dimensional space approach. This complicated structure with the peak and the dip was also obtained by Hai, Peeters, and Devreese in Ref. 20, where detailed theoretical calculations were performed.

A comparison between our results and calculations by Hai, Peeters, and Devreese²⁰ (HPD model) and by Smondyrev, Gerlach, and Dzero²¹ (SGD model) for a GaAs-Ga_{0.7}Al_{0.3}As quantum well is shown in Figs. 3(a) and 3(b). For the case of the energy shift the agreement is quite apparent. The maximal discrepancy between the tree models

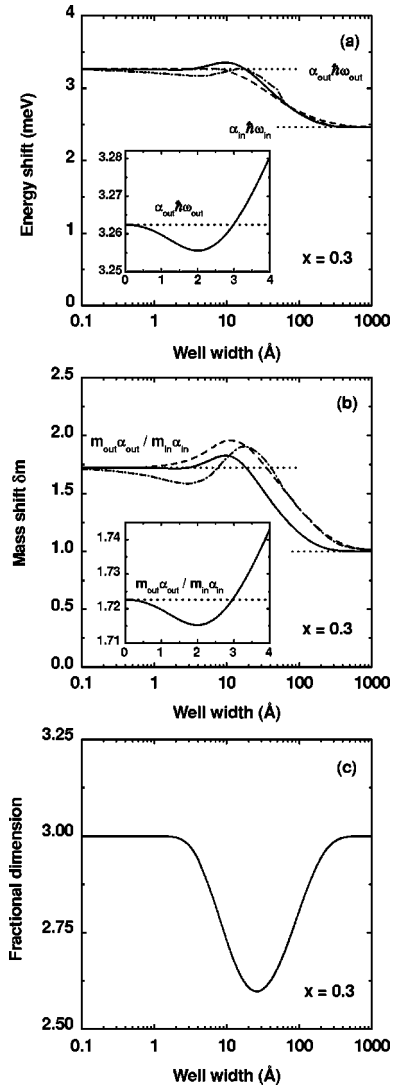


FIG. 3. Same as in Fig. 2, but now assuming material parameters as used in Refs. 10 and 11. Solid curves correspond to the present fractional-dimensional results, while dashed and dash-dotted lines correspond to the calculations by Smondyrev, Gerlach, and Dzero (Ref. 21) and by Hai, Peeters, and Devreese (Ref. 20), respectively.

is about 0.12 meV. One also can appreciate in Fig. 3(a) that the agreement between our results and the HPD model is better than that between the HPD and the SGD models in the regions $L_w \leq 3 \text{ \AA}$ and $L_w \geq 12 \text{ \AA}$. On the other hand, for the case of the mass shift [see Fig. 3(b)] the agreement between our results and the HPD model is better only for $L_w \leq 12 \text{ \AA}$. It is worth remarking that, as a difference with the SGD model,²¹ our simple fractional-dimensional space approach reproduces the structure with the peak and the dip predicted by the more detailed (and much more complicated) calculations within the HPD model.²⁰

The fractional dimension corresponding to our results in Figs. 3(a) and 3(b) is displayed in Fig. 3(c) as a function of the well width. The behavior is quite similar to that of the curve in Fig. 3(c). In fact Figs. 2 and 3 correspond to the same structure, i.e., a GaAs-Ga_{0.7}Al_{0.3}As quantum well.

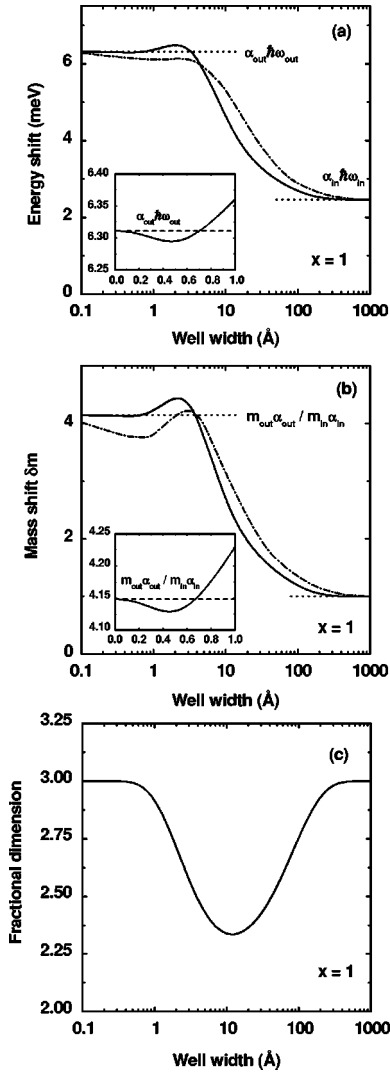


FIG. 4. Same as in Fig. 3, but for an Al concentration in the barrier $x=1$. Solid curves correspond to the present fractional-dimensional results, while dash-dotted lines correspond to the calculations by Hai, Peeters, and Devreese (Ref. 20).

However, for the computation of Fig. 2 the values of the material parameters were assumed as defined by Smondyrev, Gerlach, and Dzero in Ref. 21, while for Fig. 3 identical parameters as taken by Hai, Peeters, and Devreese²⁰ were used.

The polaronic corrections and the fractional dimension as functions of the well width for a GaAs-GaAlAs quantum well are displayed in Fig. 4. An overall agreement between our results (solid lines) and those of the HPD model (dash-dotted lines) can be appreciated in Figs. 4(a) and 4(b), although now the discrepancies between both calculations are larger than in the case of small Al concentration in the barrier (see also Fig. 3).

By comparing Fig. 3 and Fig. 4 one can study the influence of the Al concentration in the barrier on the polaronic corrections. Although the structure of the curves (with a peak and a dip for the cases of the energy and mass shifts) is conserved, one can see that the increase in the Al concentration in the well barrier produces a shift in the positions of the

peaks and dips of the polaronic corrections as well as in the position of the maximum of the fractional dimension to smaller well widths. Notice that this behavior is predicted by both the fractional-dimensional space and the HPD approaches.

In the HPD model^{10,11} the peaks and dips appear as a consequence of the competition between the contributions due to the half-space, interface, and slab phonon modes. Our simple model deals with only bulklike phonon modes and cannot give a detailed description of the physical origin of the peaks and dips of the polaronic corrections in the actual system. However, an analysis of the behavior of the peaks and dips in the effective fractional-dimensional environment can contribute to the understanding of the situation in the real physical system.

We note that although our model deals with only bulklike phonons, these phonons are characterized by parameters whose values are averaged through the heterostructure. This means that, in some way, we are taking into account the interaction with the half-space, interface, and slab phonon modes. Thus, for instance, for very narrow quantum wells, the parameters characterizing the bulk phonons in the effective fractional-dimensional system coincide with those corresponding to the half-space phonon modes in the actual system (notice that for very narrow quantum wells the most important contribution is precisely the contribution corresponding to the half-space phonon modes). Similarly, the fractional-dimensional bulk phonons can be associated, somehow, with interface and slab phonon modes in the cases of mean and large well widths, respectively.

In what follows we only refer to the case of the peak and the dip of the energy shift. The analysis for the case of the mass shift is quite similar and we omit it. In order to understand the origin of the peak and the dip in the fractional-dimensional polaron binding energy, we first note that the energy shift [see Eq. (10)] depends on the factors $\alpha\hbar\omega_{LO}$ and $G_\alpha(D)$. The former does not depend on the dimension and is determined by the material parameters that the polaron “feels” in the actual system, and the latest is determined by the dimensionality of the effective system and related to the degree of *compression* of the polaron in the quantum well. Both factors are displayed in Figs. 5(a) and 5(b), respectively, as functions of the well width. By comparing the insets in Fig. 5 one can see that for quantum wells with $L_w \lesssim 2 \text{ \AA}$ the effective environment behaves as a 3D bulk with G_α being practically a constant, while the factor $\alpha\hbar\omega_{LO}$ decreases as the well width increases. Consequently, in the region $L_w \lesssim 2 \text{ \AA}$, the energy shift decreases as the well width increases. From the point of view of the real system this region can be associated with the region in which the contribution of the half-space phonon modes is the most important one. In the region $2 \text{ \AA} \lesssim L_w \lesssim 10 \text{ \AA}$, however, G_α increases faster than the decreasing rate of $\alpha\hbar\omega_{LO}$ and gives rise to an increase in the energy shift as the well width increases. This situation leads to the appearance of the dip at $L_w \approx 2 \text{ \AA}$ [see also Fig. 3(a)]. In the region $10 \text{ \AA} \lesssim L_w \lesssim 12 \text{ \AA}$ the factor G_α continues increasing, but the decreasing rate of $\alpha\hbar\omega_{LO}$ is faster, in this region, than the increase in G_α . Therefore, the energy shift again decreases as the well width increases. This

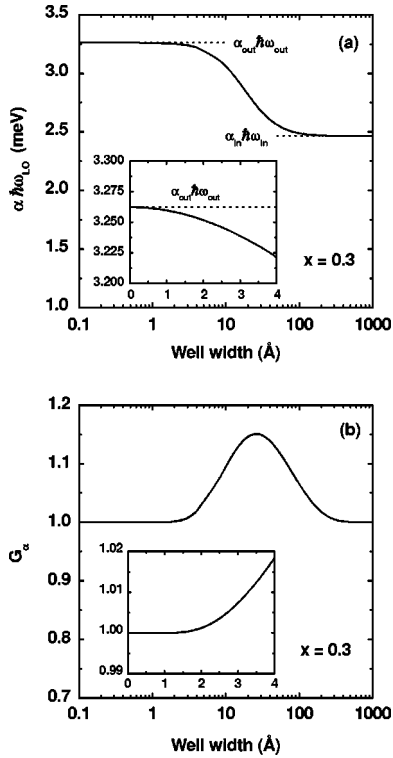


FIG. 5. Well width dependence of the factors $\alpha \hbar \omega_{LO}$ (a) and G_α (b) corresponding to a polaron confined in a GaAs-Ga_{0.7}Al_{0.3}As quantum well. The insets show a zoom-in of the curves of the corresponding factors. The material parameters have been assumed as in Ref. 20.

situation gives rise then to the presence of the peak at $L_w \approx 10$ Å [see Fig. 3(a)]. Thus the peak and the dip in the fractional-dimensional energy shift appear as a consequence of the competition between the dimensionality (i.e., the degree of *compression* of the polaron due to the confinement effects) and the material parameters “seen” by the polaron (i.e., the averaged values of the material parameters that, in some way, characterize the degree of interaction of the electron with the different phonon modes, say, half-space, interface, and slab phonon modes). From the experimental point of view, unfortunately, it seems very difficult to detect the existence of the peak and the dip of the polaron energy shift because of the smallness of the energy difference (about 0.1 meV) between them.

By taking into account the discussion above, the shift of the position of the peaks and dips of the polaronic corrections to smaller well widths when increasing the Al concentration in the barriers (compare Figs. 3 and 4) can be easily explained. The factor $\alpha \hbar \omega_{LO}$ always decreases as the well width increases [see Fig. 5(a)]; the behavior of the positions of the peak and the dip in the energy shift are therefore

essentially determined by the well width dependence of the fractional dimension. Indeed the behavior of the peak position is determined, qualitatively,⁴¹ by the behavior of the position of the minimum of the fractional dimension (i.e., the position of the maximum of G_α).

Starting from very wide quantum wells, the confinement increases (i.e., the dimension decreases) as the well width decreases until the tunneling through the barriers becomes significant. At this value of the well width the fractional dimension reaches its minimum and again increases as the well turns narrower. On the other hand, the increase in the Al molar fraction in the well barriers implies an increase in the barrier height. For higher barriers the tunneling effects become significant at smaller well widths, and this is the reason for the shift of the minimum of the fractional dimension and of the peaks of the polaronic corrections. In the case of the dip, its position is basically determined by the behavior of the point from which the fractional dimension begins to decrease (and G_α begins to increase). In a similar way of reasoning one can straightforwardly explain the corresponding shift of the dip position.

Finally, we want to note that although we have applied our fractional-dimensional space approach to the study of the polaron effects in the specific case of a rectangular quantum well, one can hope that in analogy to the fractional-dimensional models for the exciton states in semiconductor heterostructures,^{24–26} the present model for the polaronic effect can be easily generalized to the cases of other kinds of nanostructures. In fact, it has been recently shown that the fractional-dimensional space approach provides an accurate estimation of the polaronic corrections in parabolic-confined systems.⁴²

VI. CONCLUSIONS

In conclusion, the fractional-dimensional space approach was extended to the study of polarons confined in a rectangular GaAs-Ga_{1-x}Al_xAs quantum well. In this approach, the real confined “polaron + QW” system is modeled into an effective fractional-dimensional bulk in which the polaron behaves unconfined and the fractional dimension is a measure of the degree of confinement of the real system. Analytical expressions for the corresponding polaron corrections were found. These expressions allow us an estimation of the polaron binding energy and effective mass in a very simple way, avoiding the tedious and complicated calculations arising in the standard treatments. The fractional-dimensional results were shown to be in good agreement with previous more detailed calculations. The simplicity and flexibility of the proposed model suggest an easy generalization to the study of the polaron effect in other kinds of semiconductor heterostructures.

*Electronic address: amatos@mpi-halle.de

¹T. K. Mitra, A. Chatterjee, and S. Mukhopadhyay, Phys. Rep. **153**, 91 (1987).

²F. M. Peeters and J. T. Devreese, in *Solid State Physics*, edited by

F. Seitz and D. Turnbull (Academic, New York, 1984), Vol. 38.

³S. Das Sarma and B. A. Mason, Ann. Phys. (N.Y.) **163**, 78 (1985).

⁴S. Das Sarma, Phys. Rev. B **27**, 2590 (1983).

⁵S. Das Sarma and M. Stopa, Phys. Rev. B **36**, 9595 (1987).

- ⁶A. Thilagam and J. Singh, Phys. Rev. B **49**, 13 583 (1994).
- ⁷T. Tsuchiya and T. Ando, Phys. Rev. B **47**, 7240 (1993).
- ⁸R. Fuchs and K. L. Kliewer, Phys. Rev. **140**, A2076 (1965).
- ⁹K. L. Kliewer and R. Fuchs, Phys. Rev. **144**, 495 (1966); **150**, 573 (1966).
- ¹⁰X. X. Liang, Sh. W. Gu, and D. L. Lin, Phys. Rev. B **34**, 2807 (1986).
- ¹¹J. J. Licari and R. Evrard, Phys. Rev. B **15**, 2254 (1977).
- ¹²L. Wendler and R. Haupt, Phys. Status Solidi B **143**, 487 (1987).
- ¹³S. N. Klimin, E. P. Pokatilov, and V. M. Fomin, Phys. Status Solidi B **190**, 441 (1995).
- ¹⁴J. J. Licari, Solid State Commun. **29**, 625 (1979).
- ¹⁵F. Comas, C. Trallero-Giner, and R. Riera, Phys. Rev. B **39**, 5907 (1989).
- ¹⁶G. Q. Hai, F. M. Peeters, and J. T. Devreese, Phys. Rev. B **42**, 11 063 (1990).
- ¹⁷D. L. Lin, J. Phys.: Condens. Matter **3**, 4645 (1991).
- ¹⁸J. J. Shi, X. Q. Zhu, Z. X. Liu, S. H. Pan, and X. Y. Li, Phys. Rev. B **55**, 4670 (1997).
- ¹⁹M. E. Mora-Ramos and D. A. Contreras-Solorio, Physica B **253**, 325 (1998).
- ²⁰G. Q. Hai, F. M. Peeters, and J. T. Devreese, Phys. Rev. B **48**, 4666 (1993); **62**, 10 572(E) (2000).
- ²¹M. A. Smondyrev, B. Gerlach, and M. O. Dzero, Phys. Rev. B **62**, 16 692 (2000).
- ²²X. F. He, Solid State Commun. **61**, 53 (1987); **75**, 111 (1990).
- ²³X. F. He, Phys. Rev. B **42**, 11 751 (1990); **43**, 2063 (1991).
- ²⁴H. Mathieu, P. Lefebvre, and P. Christol, Phys. Rev. B **46**, 4092 (1992).
- ²⁵P. Christol, P. Lefebvre, and H. Mathieu, J. Appl. Phys. **74**, 5626 (1993).
- ²⁶P. Lefebvre, P. Christol, and H. Mathieu, Phys. Rev. B **46**, 13 603 (1992).
- ²⁷M. de Dios-Leyva, A. Bruno-Alfonso, A. Matos-Abiague, and L. E. Oliveira, J. Phys.: Condens. Matter **9**, 8477 (1997).
- ²⁸A. Matos-Abiague, L. E. Oliveira, and M. de Dios-Leyva, Phys. Rev. B **58**, 4072 (1998).
- ²⁹Q. X. Zhao, B. Monemar, P. O. Holtz, M. Willander, B. O. Fimland, and K. Johannessen, Phys. Rev. B **50**, 4476 (1994).
- ³⁰E. Reyes-Gómez, A. Matos-Abiague, C. A. Perdomo-Leiva, M. de Dios-Leyva, and L. E. Oliveira, Phys. Rev. B **61**, 13 104 (2000).
- ³¹J. Singh, D. Birkedal, V. G. Lyssenko, and J. M. Hvam, Phys. Rev. B **53**, 15 909 (1996).
- ³²A. Thilagam, Phys. Rev. B **55**, 7804 (1997).
- ³³A. Matos-Abiague, L. E. Oliveira, and M. de Dios-Leyva, Physica B **296**, 342 (2001).
- ³⁴E. Reyes-Gómez, L. E. Oliveira, and M. de Dios-Leyva, J. Appl. Phys. **85**, 4045 (1999).
- ³⁵A. Thilagam, Phys. Rev. B **56**, 4665 (1997).
- ³⁶C. Tanguy, P. Lefebvre, H. Mathieu, and R. J. Elliot, J. Appl. Phys. **82**, 798 (1997).
- ³⁷F. M. Peeters, Wu Xiaoguang, and J. T. Devreese, Phys. Rev. B **33**, 3926 (1986).
- ³⁸F. H. Stillinger, J. Math. Phys. **18**, 1224 (1977).
- ³⁹The authors used, basically, the properties of vector spaces in finding the coupling coefficient of the electron-phonon interaction. However, the fractional-dimensional space is not, in general, a vector space (Ref. 38).
- ⁴⁰A. Schäfer and B. Müller, J. Phys. A **19**, 3981 (1986).
- ⁴¹Notice that, actually, the position of the minimum of the fractional dimension does not determine quantitatively the position of the peak of the polaron energy shift (one can see in Figs. 2, 3, and 4 that the minimum of the dimensionality and the peaks of the polaron energy shift take place at different values of L_w). This is because in determining the exact position of the peak of the energy shift we have to take into account also the contribution of the factor $a\hbar\omega_{LO}$. However, the qualitative behavior of the peak position is essentially determined by the behavior of the position of the minimum of the dimensionality.
- ⁴²A. Matos-Abiague, Semicond. Sci. Technol. **17**, 150 (2002).